ANALYSIS AND DESIGN OF RETICULATED SPACE STRUCTURES

by

TARSEM LAL KOHLI

B.Sc., Punjabi University, Patiala, India, 1966

A MASTER'S REPORT

submitted in partial fulfillment of the

requirements for the degree

MASTER OF SCIENCE

Department of Civil Engineering

KANSAS STATE UNIVERSITY
Manhattan, Kansas

1970

Approved by:

Major Professor

LD
2668
R4
1970
K62
c.2

ACKNOWLEDGEMENT

The author is grateful to his adviser, Dr. Robert Ross Snell, Professor of Civil Engineering, Kansas State University, for his patience, understanding, and timely advice during the progress of this report.

A special word of thanks is due Mrs. Kimbell for her help in typing this report.

TABLE OF CONTENTS

INTRODUCTION

Formerly, reticulated shells were rarely considered because of the high cost of engineering design and analysis, joint fabrication, erection time and labor. However, with the development of new erection techniques and new joint systems, such as spheres, unistruts, and the triodetic joint (Fig. 1), they are fast gaining acceptance. New techniques for design and analysis are also being developed.

A simple reticulated shell has a curved surface composed of a single layer of prismatic members. These members intersect to form regular patterns on the surface. Some such patterns are shown in Fig. 2. The type of connection and type of member to be used are the first considerations in the establishment of any such pattern. Surface divisions are generally chosen to minimize the number of connections and the variety of members. Each lattice pattern has a particular advantage for a particular type of structure. For example, the triangular pattern of Fig. 2 (d) is best suited for the dome of Fig. 3 (a). It requires two different members in each ring and all joints may have identical angles.

In the past few years, a variety of such structures has been designed and built using the triodetic system of connecting elements and light gage cold-formed structural tubing. Apart from simple reticulated structures, structures involving additional members out of the shell surface or a complete double layer of elements have been achieved (Fig. 4). Wright[1] has presented an informative detailed

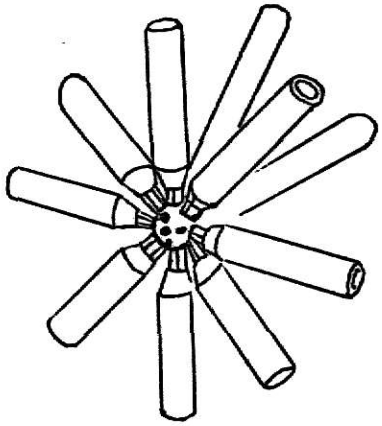

(a) Sphere

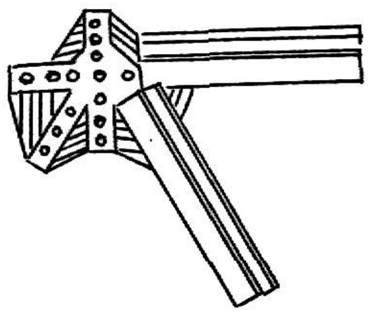

(b) Unistrut

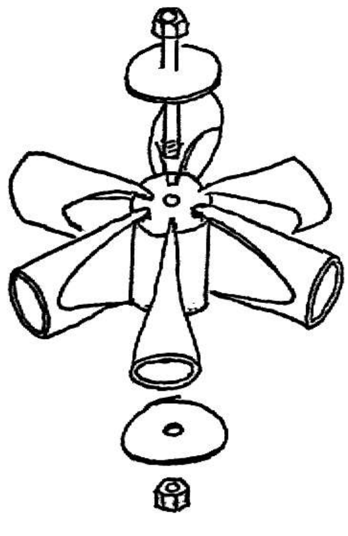

(c) Triodetic

Fig. 1. Connectors.

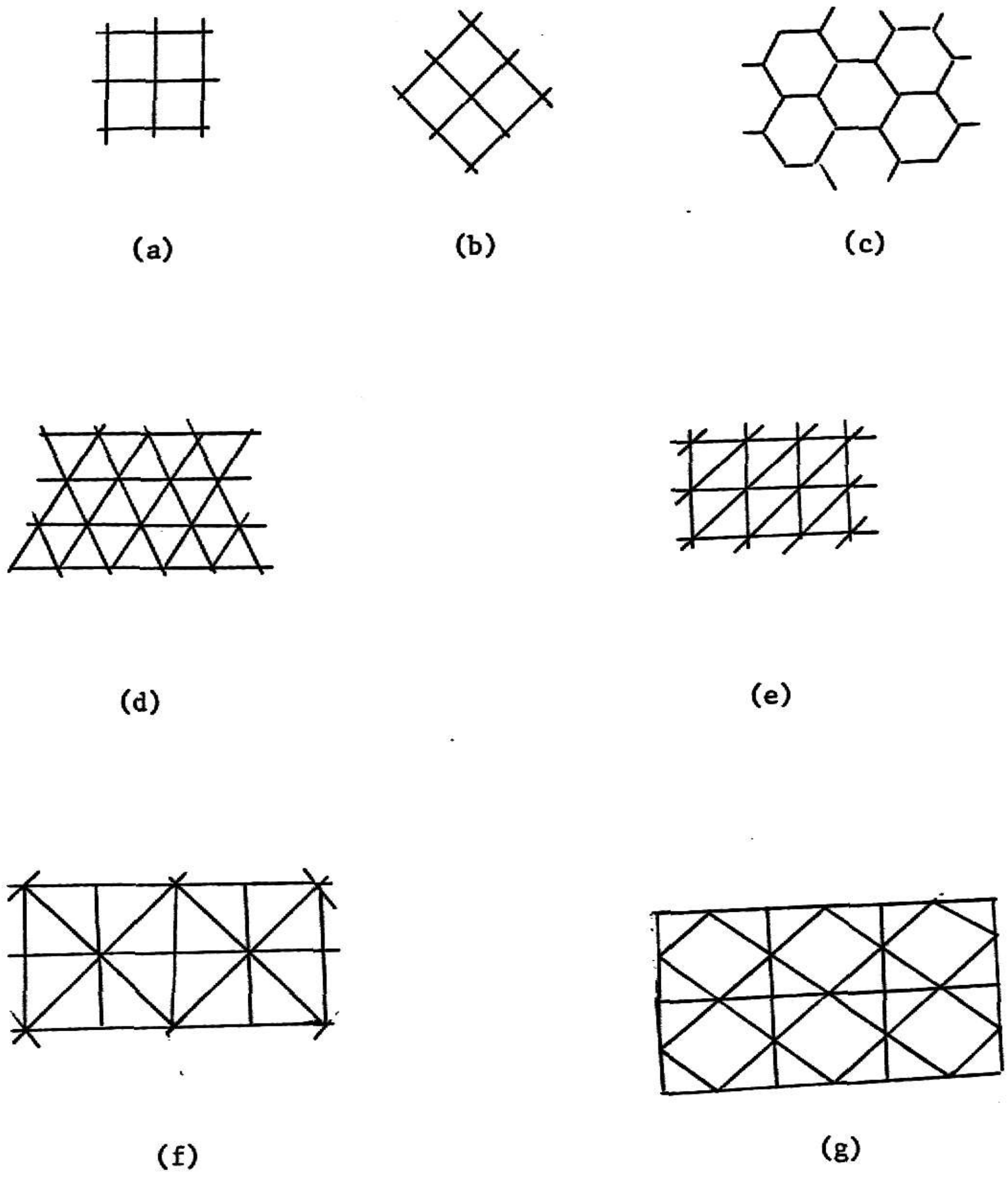

Fig. 2. Reticular patterns.

analysis of double layer domes utilizing light gage tubing. Hybrid structures have also been built. In this kind of structure there is composite structural action between a full or partial reticular framework and flat or warped skin elements that may or may not coincide with the "middle surface" of the shell and which otherwise act as cladding.

Figure 3 and Fig. 4 show some of the structures that have been built in the last few years. The trend has been to use a common connector and thus to enable each member to be optimized for minimum weight. This has resulted in more economical structures than the conventional practice of having fewer but more expensive joints. It has been determined that 250 ft. is a practical size for single layer domes from the standpoint of erection and cost. Shells larger than 300 ft., in general, should be designed as double layered. Maximum spanning capacities of up to 800 ft. and possibly more can be achieved with reticulated shell structures.[5]

With the fast-growing use of reticulated shells, many approaches for the analysis of such structures have been developed. The first and the most popular is the standard stiffness approach. Two available computer programs are STRESS[13] and FRAN[14]. FRAN has a capacity of fifteen independent loading conditions, 15,000 members, 2,000 joints and 105 structural units. The second approach has been suggested by Dean and Ugarte[7] using the concepts of discrete field mechanics. The third approach has been suggested and validated by Wright[2], Salvadori[15], and Lane[16]. They have considered the reticulated shell as a continuum.

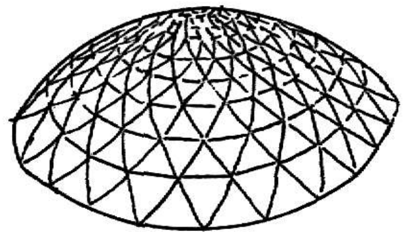

(a) Dome

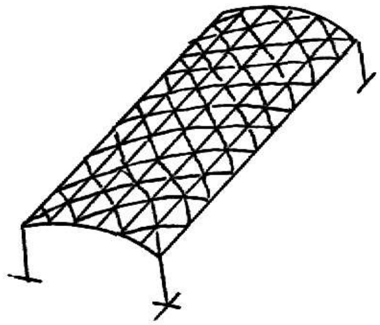

(b) Barrel

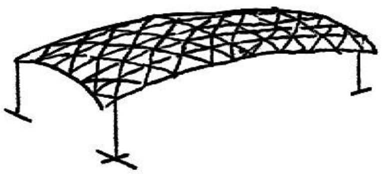

(c) Toroid

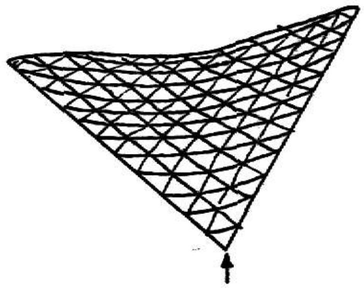

(d) Hypar

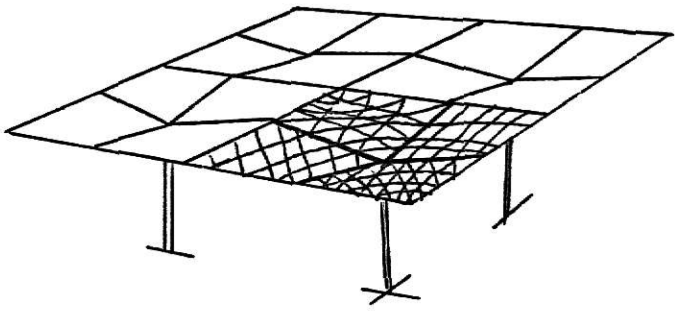

(e) Hypar-umbrella

Fig. 3. Types of reticulated shells.

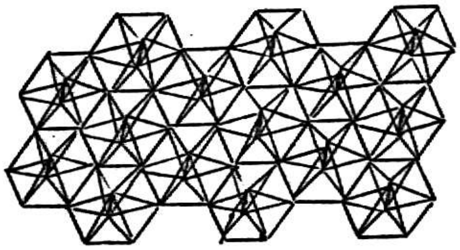

(a)

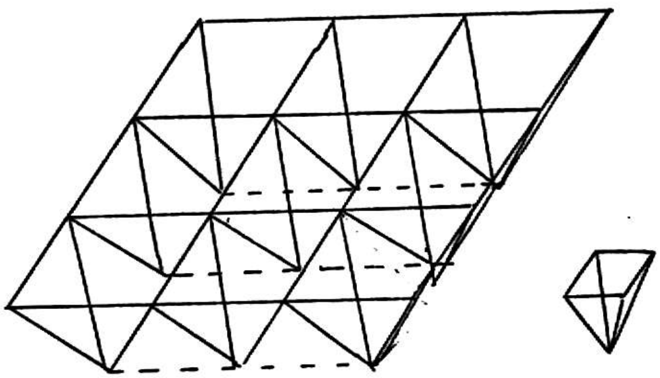

Basic unit

(b)

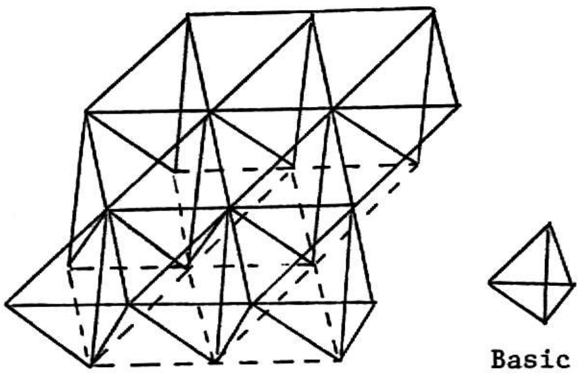

Basic unit

(c)

Fig. 4. Double-layer forms for framed shells.

Buchert[4] has derived split rigidity equations for edge effects similar to those previously used in air and spacecraft structures. The fifth approach is through the use of models.

In this report, analysis and design of "reticulated shells as continuum" will be studied with reference to the dome. Relationships between membrane forces and bar forces will be derived, elastic and physical properties of the analogous shell will be established, various buckling criteria will be given, and an example will be solved to illustrate the use of various equations.

MEMBER FORCES

Solutions for various kinds of shells under different loading conditions are available in many books on "Theory of Shells". By the membrane theory, the three components of the membrane force field N_θ, N_ϕ and $N_{\theta\phi}$ can be found at any point of the middle surface of a continuous shell. A shell may have significant bending strength but the changes in curvature and twists caused, in most cases, are so small as to be of little practical significance. Membrane theory is valid in most cases except when the edges are loaded by moments or normal shears, or when there are significant concentrated loads having components normal to the shell surface. Even in these cases, membrane theory can be used by applying corrections to the membrane solutions.

If the surface patterns of a reticulated shell (with or without cladding) are capable of resisting the forces per unit length N_θ, N_ϕ and $N_{\theta\phi}$, then it is reasonable to assume that such a shell will behave in a fashion similar to a continuous shell, at least in so far as the membrane forces are concerned. Thus, if relationships between the member forces of a reticulated shell and the membrane forces of an analogous shell can be established, many available solutions for continuous shells can be used to advantage.

Two popular patterns in the analysis and design of reticular domes are shown in Fig. 2 (d) and Fig. 2 (e). They are reproduced in Fig. 5 (a) and Fig. 5 (c).

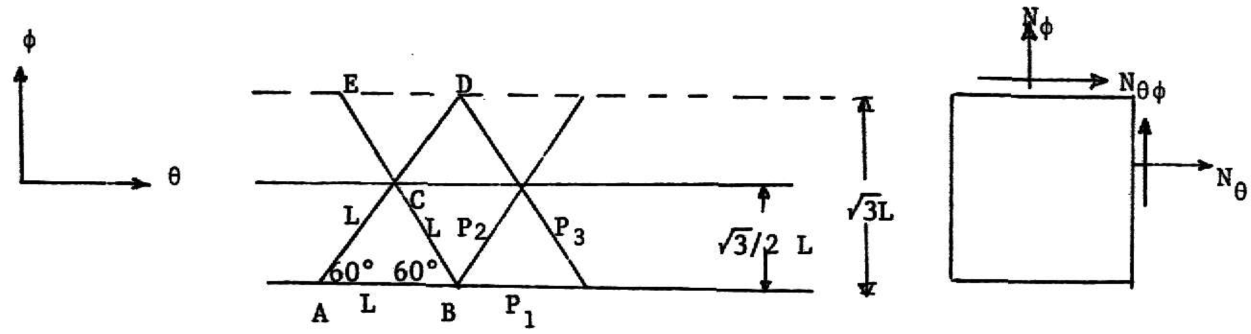

(a) Equilateral triangular grid (b) Membrane forces

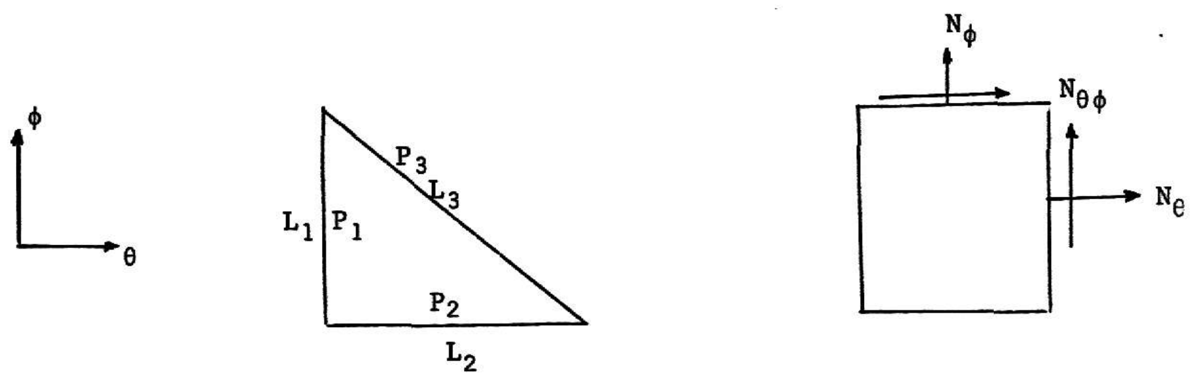

(c) Rectangular triangular grid (d) Membrane forces

Fig. 5. Equilateral and rectangular triangular grid for analysis.

Consider the pattern of Fig. 5 (a). Static equilibrium of forces on a vertical cut of length $\sqrt{3}L$ in the θ-direction gives

$$2P_1 + \frac{P_2}{2} + \frac{P_3}{2} = N\theta\sqrt{3}L$$

or

$$N_\theta = \frac{4P_1 + P_2 + P_3}{2\sqrt{3}L} \quad . \tag{1}$$

Consider equilibrium of forces in the ϕ-direction.

$$\frac{\sqrt{3}}{2} P_2 - \frac{\sqrt{3}}{2} P_3 = N_{\theta\phi}\sqrt{3}L$$

or

$$N_{\theta\phi} = \frac{P_2 - P_3}{2L} \quad . \tag{2}$$

Next consider the statical equilibrium of forces on a horizontal cut of length L in the ϕ-direction.

$$\frac{\sqrt{3}}{2} P_2 + \frac{\sqrt{3}}{2} P_3 = N_\phi L$$

or

$$N_\phi = \frac{\sqrt{3}(P_2 + P_3)}{2L} \quad . \tag{3}$$

To solve Eqns. (1), (2), (3) for P_1, P_2, P_3, multiply Eqn. (2) by $\sqrt{3}$ and add to Eqn. (3). Thus

$$\sqrt{3}N_{\theta\phi} + N_{\phi} = \frac{\sqrt{3}P_2}{L}$$

or

$$P_2 = \frac{L}{\sqrt{3}}\left(N_{\phi} + \sqrt{3}N_{\theta\phi}\right) . \tag{4a}$$

Substituting for P_2 in Eqn. (1),

$$N_{\theta\phi} = \frac{N_{\phi}}{2\sqrt{3}} + \frac{N_{\theta\phi}}{2} - \frac{P_3}{2L}$$

or

$$P_3 = \left(\frac{N_{\phi}}{2\sqrt{3}} - \frac{N_{\theta\phi}}{2}\right)2L$$

$$= \frac{L}{\sqrt{3}}\left(N_{\phi} - \sqrt{3}N_{\theta\phi}\right) . \tag{4b}$$

Next substitute for the values of P_2 and P_3 in Eqn. (1).

$$N_{\theta} = \frac{4P_1}{2\sqrt{3}L} + \frac{N_{\phi} + \sqrt{3}N_{\theta\phi}}{6} + \frac{N_{\phi} - \sqrt{3}N_{\theta\phi}}{6}$$

$$= \frac{4P_1}{2\sqrt{3}L} + \frac{N_{\phi}}{3}$$

or

$$P_1 = \frac{L}{2\sqrt{3}} (3N_\theta - N_\phi) \quad .$$

Rewriting,

$$P_1 = \frac{L}{2\sqrt{3}} (3N_\theta - N_\phi) \tag{5}$$

$$P_2 = \frac{L}{\sqrt{3}} (N_\phi + \sqrt{3}N_{\theta\phi}) \tag{6}$$

$$P_3 = \frac{L}{\sqrt{3}} (N_\phi - \sqrt{3}N_{\theta\phi}) \quad . \tag{7}$$

Equations (5), (6) and (7) give the relationships for finding the member forces, for the equilateral triangle pattern of Fig. 5 (a), from the known membrane forces of the analogous shell.

Similar relationships can be established for the pattern of Fig. 5 (c).

Consider the statical equilibrium of forces on a vertical cut of length L_1 in the θ-direction.

$$P_2 + \frac{L_2}{L_3} P_3 = L_1 N_\theta \quad . \tag{8a}$$

Considering equilibrium in the ϕ-direction,

$$P_3 \frac{L_1}{L_3} = L_1 N_{\theta\phi} \quad . \tag{8b}$$

Consider the statical equilibrium of forces on a horizontal cut of length

L2 in the ϕ-direction.

$$P_1 + \frac{L_1}{L_3} P_3 = N_\phi L_2 \quad . \tag{8c}$$

Equation (8b) gives

$$P_3 = L_3 N_{\theta\phi} \quad . \tag{9a}$$

Substituting for P_3 in Eqn. (8a),

$$P_2 + L_2 N_{\theta\phi} = L_1 N_\theta$$

or

$$P_2 = L_1 N_\theta - L_2 N_{\theta\phi} \quad . \tag{9b}$$

Also substituting for P_3 in Eqn. (9c),

$$P_1 = N_\phi L_2 - \frac{L_1}{L_3}(L_3 N_{\theta\phi})$$

$$= L_2 N_\phi - L_1 N_{\theta\phi} \quad . \tag{9c}$$

Rewriting Eqns. (9a), (9b) and (9c),

$$P_1 = L_2 N_\phi - L_1 N_{\theta\phi} \quad , \tag{10}$$

$$P_2 = L_1 N_\theta - L_2 N_{\theta\phi} \quad , \tag{11}$$

$$P_3 = L_3 N_{\theta\phi} \quad . \tag{12}$$

The above two cases show the simplicity of establishing the relationships between the member forces and the membrane force. Similar relationships can be established for any other reticular pattern by following the method indicated above. It is important to note that relationships (5), (6), (7), (10), (11) and (12) are independent of member sections and are statically determinate.

ELASTIC PROPERTIES OF THE ANALOGOUS SHELL

To establish a homogeneous shell that is analogous to the reticulated shell, its elastic and physical properties must be established. The elastic properties of the analogous shell are known if Hook's law can be expressed for its "material". Given that the grid members are homogeneous and linearly elastic, it is reasonable to assume that the material of the analogous shell is homogeneous and linearly elastic for any of the patterns shown in Fig. 2. In general, as the grid members running in different directions can have different sections, it is not reasonable to assume that the "material" is isotropic. The joints are considered to be structurally adequate and of zero dimension on the shell surface. Although it is questionable whether the joint characteristics can appreciably affect the shell stability, still the relationships developed in this case may readily be modified to suit the actual joint behavior.

Consider the array shown in Fig. 6. It has members of two different sections. Member 1 has area of cross section A_1 and moment of inertia I_1. Members 2 and 3 have area of cross section A_2 and moment of inertia I_2. The material of the analogous shell is considered to be homogeneous, linearly elastic and anisotropic.

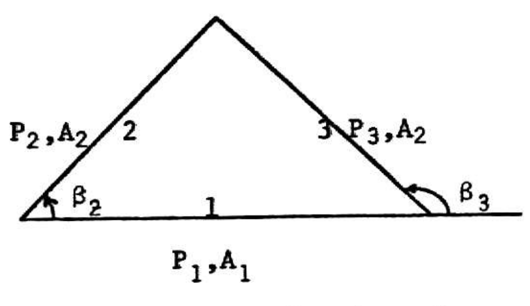

Fig. 6. Equilateral triangular grid.

Hook's law can be written as

$$\varepsilon_\theta = \frac{\sigma_\theta}{E'_\theta} - \nu'_\theta \frac{\sigma_\phi}{E'_\phi} \tag{13a}$$

$$\varepsilon_\phi = \frac{\sigma_\phi}{E'_\phi} - \nu'_\phi \frac{\sigma_\theta}{E'_\theta} \tag{13b}$$

$$\gamma_{\theta\phi} = \frac{\tau_{\theta\phi}}{G'} \tag{13c}$$

where

ε_θ = normal strain in θ-direction,

ε_ϕ = normal strain in ϕ-direction,

$\gamma_{\theta\phi}$ = shear strain,

σ_θ = normal stress in θ-direction,

σ_ϕ = normal stress in ϕ-direction,

$\tau_{\theta\phi}$ = shear stress,

ν'_θ = Poisson's ratio of the analogous shell in θ-direction,

ν'_ϕ = Poisson's ratio of the analogous shell in ϕ-direction,

E'_θ = Modulus of Elasticity of the analogous shell in the θ-direction,

E'_ϕ = Modulus of Elasticity of the analogous shell in the ϕ-direction,

G' = shear modulus of the analogous shell.

To solve for σ_θ, σ_ϕ, $\tau_{\theta\phi}$ from Eqns. (13a), 13b) and (13c), multiply Eqn. (13b) by ν'_θ and add to Eqn. (13a).

$$(\varepsilon_\theta + \nu'_\theta \varepsilon_\phi) = \frac{\sigma_\theta}{E'_\theta}(1 - \nu'_\theta \nu'_\phi)$$

or

$$\sigma_\theta = \frac{E'_\theta(\varepsilon_\theta + \nu'_\theta \varepsilon_\phi)}{(1 - \nu'_\theta \nu'_\phi)} \quad . \tag{14a}$$

Similarly multiply Eqn.(13a) by ν'_ϕ and add to Eqn. (13b).

$$\sigma_\phi = \frac{E'_\phi(\varepsilon_\phi + \nu'_\phi \varepsilon_\theta)}{(1 - \nu'_\theta \nu'_\phi)} \quad . \tag{14b}$$

Equation (13c) can be rewritten as

$$\tau_{\theta\phi} = G'\gamma_{\theta\phi} \quad .$$

Next consider the deformation of the grid shown in Fig. 6.

$$\varepsilon 1 = \frac{P_1}{A_1 E} \tag{15a}$$

$$\varepsilon_2 = \frac{P_2}{A_2 E} \tag{15b}$$

$$\varepsilon 3 = \frac{P_3}{A_2 E} \quad , \tag{15c}$$

where ε_1, ε_2, ε_3 are the strains in members 1, 2 and 3, respectively, and E is the modulus of elasticity of the material of the members.

Knowing the strains ε_1, ε_2, ε_3 in any three directions, ε_θ, ε_ϕ, $\gamma_{\theta\phi}$ can be found by the use of the following equations given by Perry and Lisner[17].

$$\varepsilon_1 = \frac{\varepsilon_\theta + \varepsilon_\phi}{2} + \frac{\varepsilon_\theta - \varepsilon_\phi}{2} \cos 2\beta_1 + \frac{\gamma_{\theta\phi}}{2} \sin 2\beta_1 \quad , \tag{16a}$$

$$\varepsilon_2 = \frac{\varepsilon_\theta + \varepsilon_\phi}{2} + \frac{\varepsilon_\theta - \varepsilon_\phi}{2} \cos 2\beta_2 + \frac{\gamma_{\theta\phi}}{2} \sin 2\beta_2 \quad , \tag{16b}$$

$$\varepsilon_3 = \frac{\varepsilon_\theta + \varepsilon_\phi}{2} + \frac{\varepsilon_\theta - \varepsilon_\phi}{2} \cos 2\beta_3 + \frac{\gamma_{\theta\phi}}{2} \sin 2\beta_3 \quad , \tag{16c}$$

where β_1, β_2, β_3 are the angles which the members make with the positive direction of the chosen θ-axis, Fig. 6.

In this case, $\beta_1 = 0$; $\beta_2 = 60°$; $\beta_3 = 120°$ substituting for β_1, β_2, β_3 in Eqn. (16).

$$\varepsilon_1 = \frac{\varepsilon_\theta + \varepsilon_\phi}{2} + \frac{\varepsilon_\theta - \varepsilon_\phi}{2} = \varepsilon_\theta \quad , \tag{17a}$$

$$\varepsilon_2 = \frac{\varepsilon_\theta + \varepsilon_\phi}{2} - \frac{1}{2}\frac{(\varepsilon_\theta - \varepsilon_\phi)}{2} + \frac{\sqrt{3}}{2}\frac{\gamma_{\theta\phi}}{2} \tag{17b}$$

$$\varepsilon_3 = \frac{\varepsilon_\theta + \varepsilon_\phi}{2} - \frac{1}{2}\frac{(\varepsilon_\theta - \varepsilon_\phi)}{} - \frac{\sqrt{3}}{2}\frac{\gamma_{\theta\phi}}{2} \quad . \tag{17c}$$

From Eqn. (17a),

$$\varepsilon_\theta = \varepsilon_1 \quad . \tag{18a}$$

Subtract Eqn. (17c) from Eqn. (17b).

$$\varepsilon_2 - \varepsilon_3 = \frac{\sqrt{3}}{2}\gamma_{\theta\phi} \quad ,$$

or

$$\gamma_{\theta\phi} = \frac{2}{\sqrt{3}}(\varepsilon_2 - \varepsilon_3) \quad . \tag{18b}$$

Add Eqns. (16b) and (16c) and substitute for ε_θ from Eqn. (18a).

$$\varepsilon_2 + \varepsilon_3 = \varepsilon_\theta + \varepsilon_\phi - \frac{\varepsilon_\theta - \varepsilon_\phi}{2}$$

$$= \frac{\varepsilon_\theta}{2} + \frac{3\varepsilon_\phi}{2} ,$$

or

$$\varepsilon_\phi = \frac{-\varepsilon_\theta + 2\varepsilon_2 + 2\varepsilon_3}{3} ,$$

or

$$\varepsilon_\phi = \frac{-\varepsilon_1 + 2\varepsilon_2 + 2\varepsilon_3}{3} . \tag{18c}$$

Substituting for ε_1, ε_2, ε_3 from Eqn. (15) in Eqn. (18),

$$\varepsilon_\theta = \frac{P_1}{A_1E} , \tag{19a}$$

$$\varepsilon_\phi = \frac{-P_1}{3A_1E} + \frac{2P_2}{3A_2E} + \frac{2P_3}{3A_2E} , \tag{19b}$$

$$\gamma_{\theta\phi} = \frac{2(P_2 - P_3)}{\sqrt{3}A_2E} . \tag{19c}$$

Equations (19) gives strains in the θ, ϕ-directions and shear strain in terms of the member forces. The elastic constants in Eqns. (13) and (14) can now be determined between Eqns. (1), (2), (3), (13) and (19).

If t^m_θ, t^m_ϕ are the membrane thicknesses of the analogous shell normal to the θ and ϕ-directions and t^m_s is the shear thickness, then the following relationships can be written.

$$\sigma_\theta = \frac{N_\theta}{t_\theta^m} \tag{20a}$$

$$\sigma_\phi = \frac{N_\phi}{t_\phi^m} \tag{20b}$$

$$\tau_{xy} = \frac{N_{\theta\phi}}{t_s^m} \quad . \tag{20c}$$

It can be seen from Eqn. (13a) that when

$$\sigma_\phi = 0 \quad ,$$

$$E'_\theta = \frac{\sigma_\theta}{\varepsilon_\theta} \quad . \tag{21a}$$

Using Eqn. (20a), Eqn. (21a) can be written as

$$E'_\theta = \frac{N_\theta}{t_\theta^m \varepsilon_\theta} \quad .$$

Substituting from Eqn. (1),

$$\sigma_\theta = \frac{(4P_1 + P_2 + P_3)}{2\sqrt{3}Lt_\theta^m} \quad . \tag{21b}$$

Since $\sigma_\phi = 0$ was assumed, from Eqns. (3) and (20b),

$$\sigma_\phi = \frac{\sqrt{3}(P_2 + P_3)}{2Lt_\phi^m} = 0 \quad ,$$

or

$$P_2 + P_3 = 0 \quad .$$

Substituting this in Eqn. (21b),

$$\sigma_\theta = \frac{2P_1}{\sqrt{3}Lt_\theta^m} \quad .$$

Equation (21a), after substituting for ε_θ and σ_θ, can thus be written as

$$E'_\theta = \frac{2P1}{\sqrt{3}Lt_\theta^m} x \frac{A_1E}{P_1}$$

$$= \frac{2A_1E}{\sqrt{3}Lt_\theta^m} \quad . \tag{21c}$$

Similarly, Eqn. (13b) can be written as

$$E'_\phi = \frac{\sigma_\phi}{\varepsilon_\phi} \quad ,$$

when

$$\sigma_\theta = 0 \quad . \tag{21d}$$

From Eqns. (1), (20b), and (21d),

$$\sigma_\theta = \frac{N_\theta}{t_\theta^m}$$

$$= \frac{4P_1 + P_2 + P_3}{2\sqrt{3}Lt_\theta^m} = 0 \quad ,$$

or

$$4P_1 = - (P_2 + P_3) \quad . \tag{21e}$$

From Eqns. (3) and (20b),

$$\sigma_\phi = \frac{\sqrt{3}(P_2 + P_3)}{2Lt^m_\phi} \quad . \tag{21f}$$

Substituting from Eqn. (21e),

$$\sigma_\phi = \frac{\sqrt{3}}{2Lt^m_\phi}(-4P_1) \quad . \tag{21g}$$

Equation (19b), after substituting from Eqn. (21e), becomes

$$\varepsilon_\phi = \frac{-P_1}{3A_1E} - \frac{8P_1}{3A_2E}$$

$$= \frac{-P_1(A_2 + 8A_1)}{3A_1A_2E} \quad . \tag{21h}$$

Substituting Eqns. (21g) and (21h) into Eqn. (21d),

$$E_\phi{}' = \frac{\sqrt{3}(-4P_1)}{2Lt^m_\phi} \times \frac{3A_1A_2E}{-P_1(A_2 + 8A_1)}$$

$$= \frac{6\sqrt{3}A_1A_2E}{Lt^m_\phi(A_2 + 8A_1)}$$

$$= \frac{6\sqrt{3}A_2E}{Lt^m_\phi(8 + \frac{A_2}{A_1})} \quad . \tag{21i}$$

Equation (13c) can be written as

$$G' = \frac{\tau_{\theta\phi}}{\gamma_{\theta\phi}} \quad . \tag{21j}$$

From Eqn. (20c),

$$\tau_{\theta\phi} = \frac{N_{\theta\phi}}{t_s^m} \quad . \tag{21k}$$

Substituting from Eqn. (2),

$$\tau_{\theta\phi} = \frac{P_2 - P_3}{2Lt_s^m} \quad . \tag{21l}$$

Substituting from Eqns. (19c) and (21j) in Eqn. (13c),

$$G' = \frac{P_2 - P_3}{2Lt_s^m} \times \frac{\sqrt{3}A_2E}{2(P_2 - P_3)}$$

$$= \frac{\sqrt{3}A_2E}{4Lt_s^m} \quad . \tag{21m}$$

Equations (21c), (21i) and (21m) give expressions for elastic constants E_θ', E_ϕ' and G' for the analogous shell. For $\varepsilon_\theta = 0$, Eqn. (13a) gives

$$\nu'_\theta = \frac{\sigma_\theta}{E'_\theta} \frac{E'_\phi}{\sigma_\phi} \quad . \tag{22a}$$

Substituting Eqns. (20a), (20b), (21c) and (21i),

$$\nu'_\theta = \frac{N_\theta}{t_\theta^m} \times \frac{t_\phi^m}{N_\phi} \times \frac{6\sqrt{3}A_2E}{Lt_\phi^m(8 + \frac{A_2}{A_1})} \times \frac{3Lt_\theta^m}{2A_1E}$$

$$= \frac{9N_\theta A_2}{N_\phi(8 + \frac{A_2}{A_1})A_1} \quad . \tag{22b}$$

As

$$\varepsilon_\theta = \frac{P_1}{A_1 E} = 0 \quad ,$$

$$\therefore P_1 = 0 \quad .$$

Substituting $P_1 = 0$ in Eqns. (1) and (3),

$$N_\theta = \frac{P_2 + P_3}{2\sqrt{3}L} \tag{22c}$$

and

$$N_\phi = \frac{\sqrt{3}\,(P_2 + P_3)}{2L} \quad . \tag{22d}$$

Substitute Eqns. (22c) and (22d) in Eqn. (22b).

$$\nu'_\theta = 9 \times \frac{(P_2 + P_3)}{2\sqrt{3}L} \times \frac{2L}{\sqrt{3}(P_2 + P_3)} \times \frac{A_2}{(8 + \frac{A_2}{A_1})A_1}$$

$$= \frac{3A_2}{(8 + \frac{A_2}{A_1})A_1}$$

$$= \frac{1}{3} \times \frac{9A_2}{(8A_1 + A_2)} \quad . \tag{22e}$$

Similarly, when $\varepsilon_\phi = 0$,

$$\nu'_\phi = \frac{\sigma_\phi E'_\theta}{E'_\phi \sigma_\theta} \quad . \tag{22f}$$

From Eqn. (19b),

$$\varepsilon_\phi = \frac{-P_1}{3A_1E} + \frac{2P_2}{3A_2E} + \frac{2P_3}{3A_2E} \quad .$$

As $\varepsilon_\phi = 0$, therefore

$$P_2 + P_3 = \frac{P_1A_2}{2A_1} \quad . \tag{22g}$$

Substituting from Eqns. (20a), (20b), (21c) and (21i) in Eqn. (22f),

$$\nu'_\phi = \frac{N_\phi}{t^m_\phi} \times \frac{t^m_\theta}{N_\theta} \times \frac{2A_1E}{\sqrt{3}Lt^m_\theta} \times \frac{Lt^m_\phi(8 + \frac{A_2}{A_1})}{6\sqrt{3}A_2E}$$

$$= \frac{N_\phi}{N_\theta} \times \frac{1}{9}\frac{(8A_1 + A_2)}{A_2} \quad . \tag{22h}$$

Substituting Eqn. (22g) into Eqns. (1) and (3),

$$N_\theta = \frac{4P_1 + \frac{P_1A_2}{2A_1}}{2\sqrt{3}L}$$

$$= \frac{P_1(8A_1 + A_2)}{4A_1\sqrt{3}L} \quad , \tag{22i}$$

and

$$N_\phi = \frac{\sqrt{3}}{2L}\frac{P_1A_2}{2A_1}$$

$$= \frac{\sqrt{3}P_1A_2}{4LA_1} \quad . \tag{22j}$$

Substituting Eqns. (22i) and (22j) into Eqn. (22h),

$$\nu'_{\phi} = \frac{\sqrt{3}}{4}\frac{P_1A_2}{LA_1} \times \frac{4A_1\sqrt{3}L}{P\ (8A_1 + A_2)} \times \frac{1}{9}\frac{(8A_1 + A_2)}{A_2}$$

$$= \frac{1}{3} \ . \tag{22k}$$

Equations (22e) and (22k) give the relationships for the Poisson's Ratios ν'_{θ} and ν'_{ϕ} for the material of the analogous shell.

By a similar procedure, the elastic properties of the analogous shell for any pattern of a reticulated shell can be established. For an equilateral triangle pattern in which all members have the same area of cross-section A, Eqns. (21c), (21i), (21j), (22e) and (22k) can be written as

$$E'_{\theta} = \frac{2AE}{\sqrt{3}Lt^m_{\theta}} \ , \tag{23a}$$

$$E'_{\phi} = \frac{2AE}{\sqrt{3}Lt^m_{\phi}} \ , \tag{23b}$$

$$G' = \frac{\sqrt{3}AE}{4Lt^m_s} \ , \tag{23c}$$

$$\nu'_{\theta} = \frac{1}{3} \ , \tag{23d}$$

$$\nu'_{\phi} = \frac{1}{3} \ . \tag{23e}$$

If $t^m_{\theta} = t^m_{\phi} = t^m_s$, then

$$G' = \frac{E'_\theta}{2(1 + \nu_\theta)} = \frac{E'_\phi}{2(1 + \nu'_\phi)} \tag{24}$$

and $E'_\theta = E'_\phi = E'$. Thus, this case of an equilateral triangle with members having the same area of cross section is essentially an isotropic case having the following properties:

$$E' = \frac{2AE}{\sqrt{3}Lt^m} , \tag{25}$$

$$G' = \frac{E'}{2(1 + \nu)} = \frac{\sqrt{3}AE}{4Lt^m} , \tag{26}$$

$$\nu = \frac{1}{3} . \tag{27}$$

t^m = membrane thickness of the isotropic analogous shell.

PHYSICAL PROPERTIES

A reticulated shell is believed to possess both axial stiffness and bending stiffness. Thus, in general, it has two membrane thicknesses and two bending thicknesses. A dichotomy exists in this regard as Wright[2] has given two thicknesses and two moduli of elasticity which are based entirely on member rigidities. This has no effect when Membrane and Bending actions are considered separately, but the results show considerable variance when both these actions are combined. Herein, the physical properties will be established based on the split rigidity concept.

Membrane Thicknesses

Considering Eqn. (21c) and assuming $E'_\theta = E$,

$$t^m_\theta = \frac{2A_1}{\sqrt{3}L} \quad . \tag{28}$$

Similarly, considering Eqn. (21i) and taking $E'_\phi = E$,

$$t^m_\phi = \frac{6\sqrt{3}A_2}{L(8 + \frac{A_2}{A_1})} \quad . \tag{29}$$

For the analogous shell, Equations (28) and (29) give the membrane thicknesses in the θ-direction and ϕ-direction, respectively.

Bending Thicknesses

Consider the grid of Fig. 6 subjected to pure bending.

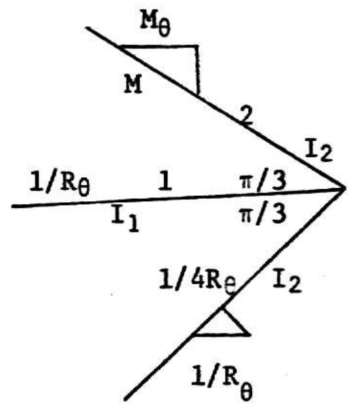

(a) Moments due to R_θ

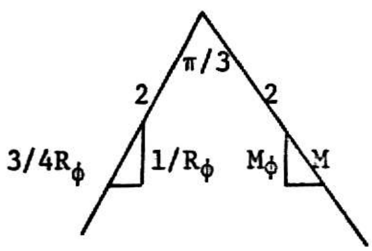

(b) Moments due to R_ϕ

Fig. 7. Bending deformations.

If R_θ is the radius of curvature in the θ-direction, then R_θ is the radius of curvature in element 1 and $4R_\theta$ in the other element, Fig. 7 (a). The corresponding moments induced in members 1 and 2 are $\frac{EI_1}{R_\theta}$ and $\frac{EI_2}{4R_\theta}$, respectively. Moment $\frac{EI_2}{4R_\theta}$ in member 2 has a component $\frac{EI_2}{8R_\theta}$ in the θ-direction.

In a repeating array of length $\sqrt{3}L$, two elements of each type cause the total moment. Thus, unit moment in the θ-direction is given by

$$m_\theta = \left(\frac{2EI_1}{R_\theta} + \frac{EI_2}{4R_\theta}\right)\frac{1}{\sqrt{3}L}$$

$$= \frac{E\,(8I_1 + I_2)}{4\sqrt{3}R_\theta L} \quad . \tag{30}$$

A radius of curvature R_ϕ, in the ϕ-direction, causes a radius of curvature $\frac{4R_\phi}{3}$ in the member 2, Fig. 7 (b). Corresponding moments induced in member 2 are equal to $\frac{3\ EI_2}{4R_\phi}$. The component of each of these moments in the ϕ-direction is equal to $3\sqrt{3}\,\frac{EI_2}{8R_\phi}$. In a repeating length L, there are two elements. Thus, unit moment in the ϕ-direction is

$$m_\phi = \frac{3\sqrt{3}EI_2}{4R_\phi L} \quad . \tag{31}$$

For bending of a plate or shell in one direction only,

$$m = \frac{D}{R} \quad , \tag{32}$$

where

m = unit moment

R = radius of curvature

and $$D = \frac{Et^3}{12(1 - \nu^2)} \quad . \tag{33}$$

Substituting Eqn. (32) into Eqn. (33) and rewriting,

$$t^3 = \frac{12\ mR(1 - \nu^2)}{E} \quad . \tag{34}$$

For bending of a shell only in the θ-direction, Eqn. (34) can be written as

$$t_\theta^{b^3} = \frac{12\ m_\theta R_\theta (1 - \nu'_\theta \nu'_\phi)}{E'_\theta} \quad . \tag{35}$$

Substituting for m_θ, ν'_ϕ from Eqns. (30) and (22k) into Eqn. (35) and assuming $\nu'_\theta = \frac{1}{3}$.

As $E'_\theta = E$ (from Eqn. (28)), therefore

$$t_\theta^{b^3} = \frac{12\ E(8I_1 + I_2)R_\theta(1 - \frac{1}{9})}{4\sqrt{3}R_\theta LE}$$

$$= \frac{8\sqrt{3}}{9}\ \frac{(8I_1 + I_2)}{L}$$

$$t_\theta^b = [\frac{8\sqrt{3}}{9}\ \frac{(8I_1 + I_2)}{L}]^{\frac{1}{3}} \quad . \tag{36}$$

For bending of the shell in the ϕ-direction only, Eqn. (34) can be written as

$$t_\phi b^3 = \frac{12\ m_\phi R_\phi (1 - \nu'_\theta \nu'_\phi)}{E'_\phi} \quad . \tag{37}$$

Substituting for m_ϕ and ν'_ϕ from Eqns. (31) and (22k) into Eqn. (37) and taking $\nu'_\theta = \frac{1}{3}$ and $E'_\phi = E$,

$$t_\phi b^3 = \frac{12 \times 3\sqrt{3} E I_2 R_\phi (1 - \frac{1}{9})}{4 R_\phi L E}$$

$$= \frac{8\sqrt{3} I_2}{L} ,$$

$$t_\phi b = (\frac{8\sqrt{3}\ I_2}{L})^{\frac{1}{3}} \quad . \tag{38}$$

Thus, the analogous shell for the equilateral triangle pattern of Fig. 6 has the following physical properties based on the assumption that $E'_\phi = E'_\theta = E$:

$$t_\theta^m = \frac{2A_1}{\sqrt{3}L} \quad , \tag{39a}$$

$$t_\phi^m = \frac{6\sqrt{3}A_2}{L(8 + \frac{A_2}{A_1})} \quad , \tag{39b}$$

$$t_\theta^b = [\frac{8\sqrt{3}}{9}\ \frac{(8I_1 + I_2)}{L}]^{\frac{1}{3}} \quad , \tag{39c}$$

$$t_\phi^b = (\frac{8\sqrt{3}\ I_2}{L})^{\frac{1}{3}} \quad . \tag{39d}$$

For the equilateral triangle pattern in which all the members are similar, $A = A_1 = A_2$ and $I = I_1 = I_2$. In this case, Eqn. (39) gives

$$t^m = t^m_\theta = t^m_\phi = \frac{2}{\sqrt{3}} \frac{A}{L} \tag{40a}$$

and

$$t^b = t^b_\theta = t^b_\phi = \left(\frac{8\sqrt{3}\, I}{L}\right)^{\frac{1}{3}} . \tag{40b}$$

BUCKLING CRITERIA

Buckling is a serious problem in the design and construction of reticulated shell structures. Recently, considerable research and analysis on the stability of such structures has been performed. Investigations of existing structures have shown that some of the structures previously designed have marginal factors of safety against buckling. Several investigators suspect that the recent failures of several structures were due to inadequate resistance against buckling. Although considerable research has been performed, there is much more work needed for the "complete art of analysis" of such structures. The results available at present can be used to design a doubly curved shell-like structure safely, efficiently, and economically.

The following factors are considered for the buckling analysis of a reticulated shell:

1. local buckling,
2. general buckling,
3. effect of edge conditions, and
4. yield strain effects.

Local Buckling

Local buckling, also known as dimple buckling, occurs when one node deflects through and the local curvature becomes negative. Very little experimental and theoretical work has been done on local buckling. Buchert[5] gives the following criteria for the local buckling of a reticulated shell, consisting of equilateral triangles with all the members having the same properties.

If the length of the member is such that

$$L^2 > 10\ R\sqrt{\frac{I}{A}}\ , \qquad (41)$$

local buckling can occur. If

$$L^2 < 10\ R\sqrt{\frac{I}{A}}\ , \qquad (42)$$

R = radius of curvature,

local buckling will not occur prior to complete loss of local curvature, and thus, failure.

Equation (42) can be used to restrict the length of members to eliminate any chances of local buckling.

General Buckling

General buckling results in the failure of the structure. It occurs over a considerable portion of the structure. Buchert[5,6] gives the following criteria for the general buckling of a framed shell.

For a reticulated shell which has the same membrane and bending thicknesses in both the directions, the wave length of the buckle is given by

$$w = 2(t^m R)^{\frac{1}{2}} \left(\frac{t^b}{t^m}\right)^{\frac{3}{4}}\ , \qquad (43)$$

w = wave length.

Critical buckling load p_{cr} is given by

$$p_{cr} = 0.366 \left(\frac{t^m}{R}\right)^2 \left(\frac{t^b}{t^m}\right)^{\frac{3}{2}} . \tag{44}$$

To consider the effect of unsymmetrical loads acting on the dome, he suggests that an equivalent pressure be calculated from the loads. That equivalent pressure should then be compared with the theoretical buckling load given by Eqn. (44), after an approximate factor of safety is applied. He suggests a factor of safety of two to be used, when designing on the basis of Eqn. (44). The equivalent pressure p_{eq} is given by

$$p_{eq} = \frac{2t^m \sigma_m}{R} , \tag{45}$$

σ_m = maximum membrane stress.

For a reticulated shell which has different membrane and bending thicknesses in each direction, Buchert[6] gives the following equation for finding p_{cr}:

$$p_{cr} = 0.183\, E\left[\frac{t^m_\theta}{R}\right]^2 \frac{J^{\frac{1}{2}} F^{\frac{1}{2}}}{Q} \left[\frac{t^b_\theta}{t^m_\theta}\right]^{\frac{3}{2}} , \tag{46}$$

where

$$B_1 = \frac{t^m_\phi}{t^m_\theta} ,$$

$$B_2 = \frac{t^b_\phi}{t^b_\theta}$$

$$J = \frac{1}{2}G^4 + G^3(1 - G) + G^2(1 - G)^2 + \frac{1}{2}G(1 - G)^3$$

$$+ \frac{1}{10}(1 - G)^4 + \frac{1}{4}G^4(B_1 - 1) + \frac{2}{3}(B_1 - 1)G^3(1 - G)$$

$$+ \frac{3}{4}(B_1 - 1)G^2(1 - G)^2 + \frac{2}{5}(B_1 - 1)G(1 - G)^3$$

$$+ \frac{1}{12}(B_1 - 1)\ (1 - G^4) \quad ,$$

$$Q = \frac{1}{2}G^2 + \frac{1}{2}G(1 - G) + \frac{1}{6}(1 - G)^2 \quad ,$$

$$F = \frac{3}{2} + \frac{9}{4}(B_2 - 1) + \frac{3}{2}(B_2 - 1)^2 + \frac{3}{8}(B_2 - 1)^3$$

$$+ \frac{1}{2}B_2^3 + \frac{3}{4}B_2^2(1 - B_2) + \frac{1}{2}B(1 - B_2)^2$$

$$+ \frac{1(1 - B_2)^3}{8} \quad ,$$

$$G = H\frac{\xi_1}{\xi_2} \quad ,$$

$$\xi_1 = [\frac{t_\theta^m}{R}]^{\frac{1}{2}}\ [\frac{t_\theta^b}{t_\theta^m}]^{\frac{3}{4}}$$

$$\xi_2 = [\frac{t_\phi^m}{R}]^{\frac{1}{2}}\ [\frac{t_\phi^b}{t_\phi^m}]^{\frac{3}{4}} \quad .$$

All of the above constants except H are known for the given shell geometry. The value of H must be determined for each case, such that p_{cr} is minimum. Different values of H (greater than 0) are assumed and p_{cr} calculated. The value of H, which gives the minimum value of p_{cr}

is the proportionality constant for the case under consideration.

Effect of Edge Conditions

Shell edge conditions affect substantially the capacity of a reticulated shell to resist buckling. The importance of edge conditions as to affecting the shell stability has been demonstrated both experimentally and theoretically. With proper edge design, buckling can be made to occur away from the edges at a higher load. Poor edge design can bring down the critical buckling load to almost zero, whereas, with proper edge conditions, a buckling load very close to the theoretical buckling load can be achieved. Buchert[5] suggests a number of ways to provide desirable edge conditions. These include increasing the effective bending thickness for a distance of approximately the buckle wave length from the edges; doubling the radius of curvature near the edge; or providing double edge rings separated by about one-fourth the wave length of the buckle, and with a moment of inertia twice that of the orthogonal members.

For a reticulated spherical shell which has the same membrane and bending thicknesses in both the directions, Buchert[5] gives the following equation to compare with Eqn. (44), to find if the edge conditions govern.

$$p_{cr} = \frac{2t^m \sigma_{cr}}{R} , \qquad (47)$$

where

σ_{cr} = critical buckling stress.

He gives the following equation to find the deflection during and prior to loading.

$$\Delta \simeq \frac{Ct^{b^3}}{3\sqrt{2}t^m} \frac{K^3}{R} \sin^2\phi_s - \frac{N_{\theta s}R}{t^m E} \tag{48}$$

where C is a constant of integration given by

$$CE = \frac{-\left(\frac{rN_{\phi s}\cos\phi_s}{A_b} + \frac{N_{\theta s}}{t^m}\right)}{\left(\frac{\sqrt{2}}{2K} + \frac{\sqrt{2}t^m r}{4K^2 A_b \sin\phi_s}\right)} \tag{49}$$

where

r = base ring radius,

ϕ_s = angle to the spring line from the shell apex,

A_b = area of the tension beam,

$N_{\theta s}$ = primary membrane circumferential stress at the spring line,

$N_{\phi s}$ = primary membrane meridional stress at the spring line,

$$K = \left[\frac{3t^m R^2}{(t^b)^3}\right]^{\frac{1}{4}} . \tag{50}$$

If $\frac{\Delta}{t^m} << 1$, then σ_{cr} in Eqn. (47) is given by

$$\frac{\sigma_{cr}R}{Et^m} = 0.41 \left(\frac{t^b}{t^m}\right)^{\frac{3}{2}} - 0.81 \frac{\Delta}{t^m} . \tag{51}$$

If $\frac{\Delta}{t^m}$ is not much less than one, the following equation is used to find σ_{cr}:

$$\frac{\sigma_{cr} R}{Et^m} = -\,0.54\,\frac{\Delta}{t^m} - 0.145\,\left[9.9\left(\frac{\Delta}{t^m}\right)^2 + 3.08\left(\frac{t^b}{t^m}\right)^3\right]^{\frac{1}{2}}$$

$$+ \left\{1.09\left(\frac{\Delta}{t^m}\right)^2 - 0.03\,\frac{\Delta}{t^m}\,\left[9.9\left(\frac{\Delta}{t^m}\right)^2 + 3.08\left(\frac{t^b}{t^m}\right)^3\right]^{\frac{1}{2}}$$

$$+ 0.359\left(\frac{t^b}{t^m}\right)^3\right\}^{\frac{1}{2}} \qquad (52)$$

Yield Strain Effects

Yield strain or yield stress of the material has a significant effect on the buckling load. After testing models in the laboratory and investigating theoretically, Buchert[6] has made the following observations:

1. Soft aluminums can reach the values given by Eqn. (44).
2. The higher strength stainless steels buckle at values that are about 1.5 times those given by Eqn. (44).
3. Annealed copper buckles at values considerably lower than those given by Eqn. (44).

DESIGN EXAMPLE

Problem: Design a reticulated spherical dome having a span of 200 ft. and a rise equal to 40 ft. Dead load is 15 psf and live load is 30 psf.

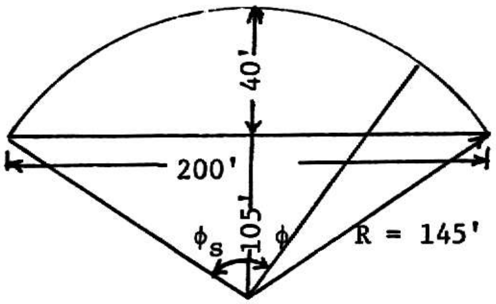

Total load = p = 45 psf = .045 ksf.

$$\text{Radius } R = \frac{(100)^2 + (40)^2}{2 \times 40}$$

$$= \frac{11600}{80}$$

$$= 145 \text{ ft.}$$

Assume that the number of members on the base circumference is equal to 120.

$$\text{Maximum length of members} = \frac{\pi \times 200}{120} = 5.024 \text{ ft.}$$

Membrane forces in a spherical shell are given by Flugge[8].

$$N_\phi = \frac{-\,pR}{1 + \cos\phi}$$

$$N_\theta = pR\left(\frac{1}{1 + \cos\phi} - \cos\phi\right)$$

$$N_{\theta\phi} = 0.$$

At the base,

$$\cos\phi = \frac{105}{145} = 0.724$$

$$N_\phi = \frac{-\,.045 \times 145}{1 + 0.724} = -\,3.785 \text{ K/ft.}$$

$$N_\theta = 0.045 \times 145 \left(\frac{1}{1 + .724} - .724\right)$$

$$= 3.785 - 4.724$$

$$= -\,0.939 \text{ K/ft.}$$

At the apex,

$$\cos\phi = 1.$$

$$N_\phi = \frac{-\,.045 \times 145}{2} = \frac{-\,6.525}{2}$$

$$= -\,3.262 \text{ K/ft.}$$

$$N_\theta = .045 \times 145\left(\frac{1}{1 + 1} - 1\right)$$

$$= -\,3.262 \text{ K/ft}$$

Maximum Member Forces

Use an equilateral triangle pattern with all members having the same cross-sectional area and triodetic joints.

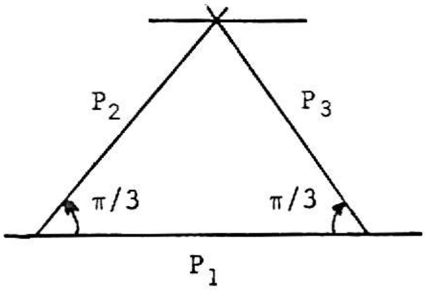

Assuming perfect joint behavior,

(refer Eqn. 5)

$$P_1 = \frac{L}{2\sqrt{3}} (3N_\theta - N_\phi)$$

$$= \frac{5.024}{2\sqrt{3}} [3(-0.939) + 3.785]$$

$$= 1.405 \text{ Kips.}$$

$$P_2 = P_3 = \frac{L}{\sqrt{3}} (N_\phi)$$ (refer Eqns. 6 and 7)

$$= \frac{5.024\ (-3.785)}{\sqrt{3}}$$

$$= -11 \text{ Kips.}$$

Use steel tubes having diameter x thickness = 4.5"x 0.157". (pg. 49, Ref. 18) (ASTM A501-68a, Hot-Formed Welded and Seamless Carbon Steel Structural Tubing, F_y = 36 ksi.)